(19) DANMARK

(10) DK/EP 3211175 T3

(12) Oversættelse af europæisk patentskrift

Patent- og Varemærkestyrelsen

(51) Int.Cl.: *E 21 B 19/00 (2006.01)* *B 66 C 13/00 (2006.01)* *B 66 D 1/00 (2006.01)*
E 21 B 19/02 (2006.01)

(45) Oversættelsen bekendtgjort den: **2022-06-20**

(80) Dato for Den Europæiske Patentmyndigheds bekendtgørelse om meddelelse af patentet: **2022-03-30**

(86) Europæisk ansøgning nr.: **16157498.3**

(86) Europæisk indleveringsdag: **2016-02-26**

(87) Den europæiske ansøgnings publiceringsdag: **2017-08-30**

(84) Designerede stater: **AL AT BE BG CH CY CZ DE DK EE ES FI FR GB GR HR HU IE IS IT LI LT LU LV MC MK MT NL NO PL PT RO RS SE SI SK SM TR**

(73) Patenthaver: **National Oilwell Varco Norway AS, Postboks 401 , Lundsiden, 4604 Kristiansand S, Norge**

(72) Opfinder: **Kyllingstad, Åge, Hogstadbakken 8, 4330 Ålgård, Norge**

(74) Fuldmægtig i Danmark: **Håmsø Patentbyrå AS, Postboks 9, NO- 4068 Stavanger, Norge**

(54) Benævnelse: **Hoisting system and method for operating the same**

(56) Fremdragne publikationer:
PL-B1- 158 970
US-A- 2 238 398
US-A- 2 565 693
US-A- 2 681 793
US-A1- 2015 275 647
US-A1- 2015 353 331

DESCRIPTION

Background

[0001] Drawworks is a common name for the actuator being used for moving the drill string up and down in the well. It consists of a multi-layer drum powered by electrical motors, a drill line running from the drum over a fast sheave near the top of the derrick, then strung several times between the crown block and the travelling block and then back down to a dead line anchor locking it to the rig structure. The drill line is a steel wire rope having a nominal diameter of typically 3,81 to 5,08 cm (1.5 to 2 inches). The fast line is the part of the drill line that runs between the drum and the fast sheave. It has a fixed length, typically 50 m, and it is more and less free to move transversally. Both the lower drum end and the upper fast sheave end represents dynamically fixed ends, making the fast line behave very similar to a string of a musical string instrument. The dimensions, resonance frequencies and excitation mechanisms are quite different, though. While a musical instrument string is set into vibrations by plucking it (guitar), by a hammer (piano) or by a bow (violin), the fast line is excited mainly by lateral motions at the drum end. Because there is very little damping of transversal drill line vibrations, large amplitudes can be the result if one of the drum spooling harmonics coincides with the natural line frequencies. In extreme cases the fast line can hit surrounding equipment and cause damages, also to itself. Large transversal vibrations are highly undesirable also because they cause excessive wear of the line and of the fast sheave. In extreme cases erroneous drum spooling can occur during hoisting operation. If the line jumps over one wrap during hoisting, it can lead to severe line damage when the next layer is filled.

[0002] To avoid large and damaging transversal line vibrations it has become common practice to install one or, and in some cases, two so-called fast line stabilizers. Such a devise is a movable mass with guide rollers mounted some distance above the drum. It is relatively free to move laterally by means of wires running over guide sheaves. Its mass and the friction in the guiding system are indented to reduce resonant vibrations and thereby hindering damages to the line or to other equipment. However, experience shows that the current type and placement of stabilizers is not always very efficient and that severe damages can still occur, especially when the tension is low and the hoisting speed is high. The main disadvantages of current state of the art are listed below. The radial and axial directions refer to the drum axis.

1. 1. The stabilizer guide system represents virtually no damping in the radial direction of transversal vibrations.
2. 2. The damping in the axial direction is dominated by non-linear Coulomb friction in the sheaves of its guide system. The ratio of friction force to inertia forces for this kind damping decreases with the speed amplitude. This feature is far from optimal because the largest vibrations in general need the highest damping.
3. 3. Poor damping of axial vibrations also means higher fluctuations of the fleet angle, defined as the angle between the fast line tangent and the perfectly straight line between the drum center and the fast sheave. Higher fleet angle fluctuations imply excessive

forces and wear on the sides of the sheave groove.

4. 4. The stabilizer system occupies a lot of space in the derrick because the comprehensive guide system with tensioning wires and sheaves need space to accommodate the large axial motion.
5. 5. The system is relatively expensive to install and to maintenance.
6. 6. Their poor performance and the risk of erroneous drum spooling sometimes cause the maximum hoisting speeds to be limited, which in turn, means poor rig performance and high costs.

[0003] Some or all of these disadvantages are observed in the following documents. Document US 2 565 693 A discloses a wire line guide for an installation in a derrick or similar structure in alignment with a run of a line leading from a drum and over a crown pulley. Document PL 158 970 B1 discloses a device damping transverse vibrations of the dead end of a cable, in particular the cable of a drill rig. And document US 2015/353331 A1 discloses a stabilizer for a line, the stabilizer including a guide for arrangement on the line to resist and/or dampen lateral motions of the line.

[0004] The invention has for its object to remedy or to reduce at least one of the drawbacks of the prior art, or at least provide a useful alternative to prior art.

[0005] The object is achieved through features, which are specified in the description below and in the claims that follow.

[0006] In a first aspect the invention relates to a hosting system for a drilling rig, the hoisting system comprising:

- a wire rope;
- a winch for pulling in and letting out said wire rope,
- a support structure, such as a derrick;
- a wire rope guiding sheave connected to the support structure, said wire rope guiding sheave being provided between said winch and a load suspension member along the wire rope; and
- one or two stabilizers for damping lateral vibrations of the wire rope between said winch and said wire rope guiding sheave, wherein, in order to increase the damping effect of the one or two stabilizers, each of the one or two stabilizers is provided closer to the wire rope guiding sheave than to the winch drum along the wire rope. Also, a first stabilizer of said one or two stabilizers comprises one or more dampers with first end(s) connected to said support structure, said first stabilizer further comprising one or more pairs of guide rollers common to each of said one or more dampers and connected to a second end of said one or more pairs of dampers, said wire rope being adapted to run between the rollers of each of said one or more pairs of guide rollers Moreover, said first stabilizer comprises a pair of dampers, wherein longitudinal axes of the two dampers are substantially perpendicularly oriented relative to each other

[0007] In a second aspect the invention relates to a method for damping lateral vibrations in a wire rope by means of a hoisting system according to the first aspect of the invention, the method comprising the steps of:

- measuring the rotational speed of a winch drum of the winch;
- measuring the tension of the wire rope between said winch and said wire rope guiding sheave; and
- calculating optimized motion characteristics, for reducing said lateral vibrations, of one or more dampers of said first stabilizer based on said measured rotational speed and tension.

[0008] Herein the wire rope will also interchangeably be referred as a line or drilling line, while the portion of the wire rope between the winch and the wire rope guiding sheave will also be referred to as the fast line. The wire rope guiding sheave will also be referred to as a fast sheave. All this is in accordance with common terminology as used in a traditional draw-works on a drilling rig. However, the invention should not be construed as limited to traditional draw-works, but could also be used in other hoisting systems using single layer winches and/or hoisting systems without the traditional stringing between the crown block and travelling block but using only a mechanical advantage of 2-3 or even direct drive between the winch and the load. One such hoisting system is disclosed in WO 2014/209131. Still, some of the advantages of the invention discussed herein may be more pronounced when used in a traditional drawworks as described above, in particular because the lateral fast line vibrations are more pronounced when the speed of the fast line is high.

[0009] In the following is described the theoretical basis for the invention and an example of a preferred embodiment illustrated in the accompanying drawings, wherein:

Fig. 1
shows simulated normalized drum-induced deflections, and their derivatives, as a function of winch drum rotation angle;

Fig. 2
shows the simulated normalized combined winch drum deflections as a function of winch drum rotation angle and the winch drum harmonics at the third layer;

Fig. 3
shows the simulated modulus of the normalized wire rope impedance as a function of frequency without and with different stabilizer provided near the winch drum;

Fig. 4
shows the results of similar simulations as in Fig. 3 but with the stabilizer provided near the wire rope guiding sheave/fast sheave;

Fig. 5

shows the results of similar simulations as in Fig. 4 but with different stabilizer damping characteristics;

Fig. 6
shows simulated modulus of the normalized wire rope impedance as a function of frequency;

Fig. 7
shows schematically a hoisting system according to the first aspect of the present invention as well as a more detailed view of one embodiment of a stabilizer as used in the hoisting system;

Fig. 8
shows schematically one embodiment of damper for a stabilizer as used in a hoisting system according to the present invention;

Fig. 9
shows simulation results of the axial wire rope deflection and fleet angle, respectively, at the winch drum and near the wire rope guiding sheave as a function of time without any stabilizer; and

Fig. 10
shows similar simulations as in Fig. 9 but with a stabilizer placed near the wire rope guiding sheave;

Theoretical basis

[0010] The theory description below is included to provide credibility and to justify that the new stabilizer concept together with its new location does represent a significant improvement as compared with current state of art. The theory first describes the main excitation mechanism for transversal vibrations. Next it describes how the line dynamics is affected by a stabilizer, both its mass, damping coefficient and location. The line dynamics are studied by two models, one simplified linear model suitable for frequency analysis and one full simulation model suitable for studying dynamics in the time domain.

[0011] As a typical but non-limiting example we shall study a standard multi-layer drum having so-called Lebus grooves. These grooves force the line of the first layer to follow a path of discrete but smooth steps, not a helical path often used for single layer drums. Two times per revolution (once every 180 degrees) the line is shifted half a pitch during a transition length of typically 30 drum degrees or 10 line diameters. Between these transition sectors the grooves are cylindrical thus representing no dynamic deflections. At the end of the first layer the radius is increased during another transition angle up to the second layer radius. When the line is spooled on the 2^{nd} layer, the axial motion is a kind of mirror of the 1^{st} layer motion. Because the line has to cross over the underlying line, the fast line is also forced to make a temporary, bell shaped radius increase at every cross-over.

[0012] A detailed description of the drum-induced line motion can be given by assuming that

1. 1. the line is perfectly circular with a radius denoted by *r,*
2. 2. the pitch, which is the c-c distance between neighbor wraps, is slightly larger than the diameter: $p > d = 2r$,
3. 3. the deflection change rate through the transition sectors is continuous and smooth.

[0013] We shall need a help variable representing the angular position of the contact line relative to the center of the underlying rope. This angle varies from $\gamma = -\gamma_0$ to $\gamma = \gamma_0 \equiv \sin^{-1}(0.5p/d)$ during the cross-over interval. One possible but no-limiting choice for the variation of this contact position is a sinusoidal contact angle variation such that

$$\gamma = \gamma_0 \sin\left(\frac{2\pi(\theta-\theta_c)}{\theta_x}\right) = \sin^{-1}\left(\frac{p}{2d}\right)\cdot\sin\left(\frac{2\pi(\theta-\theta_c)}{\theta_x}\right) \quad (1)$$

where θ_C denotes the drum rotation angle of the center of crossover and θ_X is the angular crossover length. The resulting cross-over deflections in respective axial and radial directions are

$$X = X_c + r\sin\gamma \quad (2)$$

$$R = R_1 + r\cos\gamma \quad (3)$$

[0014] Here X_C is the position at the center of the cross-over while R_1 refers to the center radius of the first layer.

[0015] The formulas above apply inside the cross-over intervals $|\theta - \theta_C| \leq 0.5\theta_X$ only, but they can easily be generalized to any drum angle of any layer. The axial line displacement at the drum is basically equal for each layer except that even layer numbers represent mirror motion of the odd layers. In contrast, the radius bump height increases with the layer number. Explicitly, the cross-over radius of any layer number, i_l can be expressed by

$$R = R_1 + (i_l - 1)r\cos\gamma \quad (4)$$

[0016] The radius changes at layer shifts can be modelled similarly by assuming that the radius in the transition from layer i_l -1 to layer i_l follows the function

$$R = R_1 + r\cot\gamma_0\sin\gamma + i_l r\cos\gamma_0 \quad (5)$$

[0017] In this equation the drum angle defining the help variable γ is the layer shift angle $\theta_{i-1,i}$.

[0018] It is convenient to define normalized motions and their first and second order derivatives, primes denoting differentiation with respect to θ :

$$X_n = \frac{X - X_{23}}{r} \quad (6)$$

$$R_n = \frac{R - R_1}{r} \quad (7)$$

$$X_n' = \frac{X'}{r} = \frac{2\pi}{\theta_x}\cos\gamma \quad (8)$$

$$R_n' = \frac{R'}{r} = -\frac{(i_l - 1)2\pi}{\theta_x}\sin\gamma \quad (9)$$

$$X_n'' = \frac{X''}{r} = -\frac{4\pi^2}{\theta_x^2}\sin\gamma \quad (10)$$

$$R_n'' = \frac{R''}{r} = -\frac{(i_l - 1)4\pi^2}{\theta_x^2}\cos\gamma \quad (11)$$

[0019] The last expressions for the derivatives are valid only inside the cross-over intervals. Outside these intervals the normalized motions are constant while the derivatives are zero, with the exception of the layer shifts. Here the first and second derivatives are obtained by differentiating equation (5).

[0020] The above functions are plotted versus the drum angle in three subplots in figure 1. The x-axis represents the angle in radians beyond the filled 2nd layer angle, here denoted by θ_{23}. The three subplots show the normalized deflections, their first derivatives and their second derivatives, respectively. The first derivatives represent the angular deviation from the tangent line while the second derivatives represent the line curvatures, or more precisely, the curvature deviation from the base curvature. The axial deflection steps are slightly larger than unity (line radius), reflecting the fact that the pitch in this example is chosen to be 2.5% larger than the line diameter. Also we have assumed that both the layer shift interval and the crossover intervals are 36 degrees.

[0021] The physical transversal speeds and accelerations of the line at its lower end can be calculated from the time derivatives of the deflections:

$$v_r = \dot{R} = r\Omega R_n' \quad (12)$$

$$v_x = \dot{X} = r\Omega X_n' \quad (13)$$

$$a_r = \ddot{R} = r\Omega^2 R_n'' \quad (14)$$

$$a_x = \ddot{X} = r\Omega^2 X_n'' \quad (15)$$

where

$$\Omega \equiv \dot{\theta} = \frac{v_l}{R} \quad (16)$$

is angular drum speed and v_l is the line speed. This line speed simply equals the block speed

times the number of line parts.

[0022] As a numerical example, consider a drum of radius of $R = 0.75m$ and a 1 ¾ " line ($r = 0.0222m$) running at a typical maximum line speed of $v_l = 25m/s$. The corresponding angular speed is $\Omega = 33.3rad/s$, corresponding to a fundamental cross-over frequency is $f_{xo} = 2\Omega/2\pi = 10.6\text{Hz}$. Maximum radial peak speed occur at the layer shift where $R'_{n,\max} = 4.5$ and equals $v_{r,max} = 3.4m/s$. Maximum radial acceleration at the 3rd layer crossovers ($R''_{n,\max} = 26.3$) is $a_{r,max} = 650m/s^2 \approx 66\text{g}$. These peak acceleration levels can be characterized as extremely high and could possibly be a cause of the high failure rates and maintenance costs of the current fast line stabilizers. Notice also that the peak acceleration increases proportionally to the line speed squared and inversely proportionally to the crossover length squared. In mathematical terms, $a_{r,\max} \propto r v_l^2 / (R\theta_x)^2$.

[0023] Anticipating the suggestion below of absorbing the line motion by dampers mounted in directions of characterized by angles ± π /4 relative to the pure radial direction, is useful to study the combined motion $R_n'\cos(\pi/4) + X_n'\sin(\pi/4) = (R_n' + X_n')/\sqrt{2}$ and its frequency components. Reference is made to figure 2. The upper subplot shows this combined speed versus the drum angle over the same drum angle interval as in figure 1. The lower subplot shows the corresponding harmonics spectrum of the third layer ($\theta > \theta_{23} + \theta_x$). Notice that the combined speed has a lower peak (3.2) at the layer shift than the pure radial speed and that the individual harmonics components are much smaller in amplitude (in the order 0.5) than the peak speed itself (approximately 3.4). The amplitudes are relatively constant up to the 10th harmonics, then they fall off and are quite small for the 20th harmonics and above. The harmonics spectra for the normalized deflection and acceleration are not included here but they can easily be obtained by respective dividing and multiplying the speed spectrum by the harmonics number. We then find that the harmonics components of the deflection fall rapidly off with frequency while the acceleration can have large high frequency components. The maximum acceleration components are found around the 10th harmonics for this particular case where the crossover angle covers 1/10 of a revolution.

[0024] The spectra discussed above apply if the drum is rotated at a constant speed on the 3rd layer. We see from the upper subplot in figure 2 that the layer shift is a nonperiodic pulse representing a continuous spectrum with all kind of frequencies.

[0025] It should also be mentioned that there are other type of excitation mechanisms that can put the fastline into transversal vibrations but are not included in the mathemati- cal models here. One such mechanism is the non-linear coupling between dynamic tension force and

transversal vibrations. When the line deflects laterally, it is slightly longer than the perfectly straight line and this elongation causes a variation in tension. The coupling also works the other way around, so that a change in tension affects the deflection. This mechanism can be quite strong, especially when the fast line is statically inclined (deviates from perfectly vertical) and has a low tension force. The gravitation induced, static deflection is nearly proportional to the inclination angle but inversely proportional to the tension. When the tension increases rapidly from a low value, for instance when stopping a downwards motion of an empty travelling block, then this mechanism can give rise to large transients line vibrations. Because the shape of the static deflection is very similar to the amplitude function of the fist harmonic vibration, it is mainly the first harmonic vibration that is excited by such stops of an inclined fast line. Other excitation mechanisms for transversal line vibrations are external derrick motion (applicable for floating rigs) and wind induced line forces. The vibrations induced by all these alternative excitation mechanisms will be equally well dampened by the new stabilizer as the drum generated vibrations discussed below.

[0026] The next step is to study how the fast line responds to drum-induced motions, and in particular, how the placement and motion characteristics of a stabilizer influence the response. The study consists of two different approaches, the first being a linear, frequency-based study and the other a time based simulation model. The second approach is a numeric and non-linear simulation model being discussed at the end of this section.

[0027] The first approach is based on the following simplifying assumptions.

1. 1. The fast line tension force, T, is constant, independent of time and position
2. 2. The damping is low but linear and comes mainly from internal, bending induced friction.
3. 3. The fast sheave is either laterally fixed or it has linear response characteristics.
4. 4. The longitudinal fast line speed, v_l, is small compared with the transversal wave propagation speed
   $c = \sqrt{T/m}$
   , m being the specific mass (mass per unit length).

[0028] Their validity is briefly discussed below. The fast line tension normally varies much during different operations, especially during accelerations of the drum motion. However, in a wide range of operations the tension is fairly constant, at least on time scales comparable with the lowest natural. The line weight will make the tension increase with height, but normally the tension force is much higher than its weight (gravitation force). Therefore first assumption is fairly well satisfied, at least for a wide range of operations. The second assumption is more questionable, mainly because the internal bending resistance is not linear but a Coulomb type friction. However, as long as it is relatively small the linear approximation is far better than neglecting damping. The third assumption is also well satisfied in normal cases. Finally, the validity of the last assumption is justified through the following numerical example. An empty

block with a top drive have a weight of typically 600 kN, corresponding to a line tension force of $T = 50kN$ if the blocks are strung with 12 line parts. A standard 1 ¾" line with a specific mass of $m = 8.44kg/m$ will then represent a transversal wave propagation speed of $c = 77m/s$. In comparison the typical maximum line speed is $v_l = 25m/s = 0.32c$. It can be shown mathematically that the effect of the longitudinal line speed has a 2nd order effect on the natural frequencies, which are all lowered by the factor

$1 - v_l^2/c^2 \approx 0.9$

. We can therefore conclude that the last assumption is fairly well satisfied even with the combination of a high longitudinal line speed and a low tension force.

[0029] The classical equation of motion for a loss-less stretch string is

$$m\frac{\partial^2 u}{\partial t^2} = T\frac{\partial^2 u}{\partial z^2} \qquad (17)$$

where u is the transversal deflection (in any of the two possible directions), t is the time variable and z is the longitudinal position along the straight line between the end points. The same equation applies also for the transversal speed, which is the time derivative of the deflection: $v = \partial u/\partial t$. For convenience, and for avoiding singularities in the response functions, we shall need some kind of damping along the line. For this size of wire ropes the damping is probably dominated by bending resistance, which is a kind of internal friction being proportional to the rate of curvature change. We shall therefore study the following equation of motion.

$$m\frac{\partial^2 v}{\partial t^2} = T\frac{\partial^2 v}{\partial z^2} - 2\tau T\frac{\partial^3 v}{\partial t \partial z^2} \qquad (18)$$

[0030] Here τ is an internal friction parameter having the dimension of time. The factor 2 is included for convenience, to achieve some simplification in subsequent equations. This kind of damping term gives a damping rate with drops rapidly with frequency. It is possible even within the frame of linearity to change the line damping characteristics by considering τ as a function of frequency and tension. But here we shall assume it is constant.

[0031] Because of the assumed linearity, Fourier analysis applies. It means that any solution can be described as a sum of independent frequency components. The general monofrequency solution to this equation is the sum of two damped waves represented by

$$v = ae^{j\omega t - jkz} + be^{j\omega t + jkz} \qquad (19)$$

[0032] Here a and b are arbitrary complex amplitudes of the waves travelling in positive and negative z-direction, respectively. Furthermore,

$j = \sqrt{-1}$

is the imaginary unit, ω is the angular frequency and k is the wave number, here assumed to have a positive real part. The two last parameters are related to each other through the equation

$$c^2\omega^2 = k^2(1 + j2\tau\omega) \qquad (20)$$

[0033] This equation is obtained by putting the first term of the general solution into the equation of motion. If the damping is small, $2\tau\omega << 1$, then the wave number can be approximated by

$$k = \frac{\omega}{c\sqrt{1 + j2\tau\omega}} \approx (1 - j\tau\omega)k_0 \tag{21}$$

where $k_0 = \omega/c$ is the loss-less wave number. In the following we shall, for convenience, omit the common time factor $\exp(j\omega t)$.

[0034] Energy transmission along a transmission line can always be expressed as the product of a forcing variable and a motion variable. In this case the motion variable is the transversal speed while the forcing variable is the line shear force expressed by

$$F = -T\frac{\partial u}{\partial z} = T\frac{jkae^{-jkz} - jkbe^{+jkz}}{j\omega} = a\zeta e^{-jkz} - b\zeta e^{jkz} \tag{22}$$

[0035] In the last expression we have introduced the characteristic impedance

$$\zeta = \frac{Tk}{\omega} = (1 - j\tau_b\omega)\sqrt{Tm} = (1 - j\tau_b\omega)mc \tag{23}$$

[0036] For a lossless line the characteristic impedance is purely real.

[0037] It is also convenient to define general mechanical impedance as the ratio of transversal force to transversal speed, applicable both to a specific location of the line and to a lumped element connected to the line. A wide class of lumped impedance elements can be characterized by its mass$M$, its damping coefficient B and the stiffness S of an optional spring. The complex Fourier representation of such an impedance element is

$$Z_s = j\omega M + Z_c \tag{24}$$

where

$$Z_c = B + \frac{S}{j\omega} \tag{25}$$

[0038] If an elastomer (rubber) type coupling is used, it can, to a fairly good approximation, be modelled with stiffness-proportional damping, that is, $B = 0$ and $S = S_0 . (1 + j\eta)$.

[0039] Here η is a hysteresis loss factor, in the range 0.15-0.3 for typical elastomer qualities.

[0040] The above single degree of freedom (DOF) lumped impedance can be generalized to include multiple masses and coupling elements between the line and a fixed point. It can be shown that the impedance of an n-DOF system can be found by the following recursion formula.

$$Z_{s,i} = j\omega M_i + \left(Z_{c,i}^{-1} + Z_{s,i-1}^{-1}\right)^{-1} \tag{26}$$

[0041] Here $Z_{c,i}$ is the coupling impedance between masses M_i and M_{i-1} and the higher index is closer to the line.

[0042] The coordinate system is here chosen so that the longitudinal location variable z equals 0 at the fast sheave and *-L* at the drum. In the general wave solution (10) above, the amplitudes *α* and *b* therefore represent the amplitudes of the incident and reflected waves, respectively. It can be shown that the reflection coefficient at the top line end (z = 0) can be expressed by the ratio

$$\frac{b}{a}=\frac{\zeta-Z_0}{\zeta+Z_0} \qquad (27)$$

where Z_0 represents the impedance of the fast sheave. Normally, when the fast sheave support is very stiff, this impedance is close to infinity, making $b = -\alpha$. If there are no impedance elements between the line position z and the top end, the impedance at the location z equals

$$Z(z)=\frac{F(z)}{v(z)}=\frac{a\zeta e^{-jkz}-b\zeta e^{jkz}}{ae^{-jkz}+be^{jkz}}=\frac{Z_0\cos(kz)+j\zeta\sin(kz)}{\zeta\cos(kz)+jZ_0\sin(kz)}\zeta \qquad (28)$$

[0043] These expressions are valid even when linear damping makes the wave number complex. A useful special case is when the fast sheave is rigidly supported ($|Z_0| = \infty$) and there are no stabilizers. The line impedance at the drum end then equals

$$Z_d\equiv Z(-L)=\frac{\cos(kL)}{j\sin(kL)}\zeta=-j\cot(kL)\zeta \qquad (29)$$

[0044] For low damping values the modulus of the normalized drum impedance, $|Z_d/\zeta|$, has high peaks at the discrete frequencies

$$f_i=\frac{\omega_i}{2\pi}=i\frac{c}{2L} \qquad (30)$$

[0045] i being a positive integer. We identify these frequencies as the natural (harmonic resonance) frequencies of the classical lossless string. With a small damping this normalized impedance can reach very high values, maybe hundred or more. The implication is that the dynamic transversal deflection and speeds can reach very high values if one the excitation frequencies, which are even multiples of the drum rotation frequency, matches one of the above string resonance frequencies.

[0046] Another interesting special case, although being difficult to implement physically, is when the top impedance matches the characteristic impedance: $Z_0 = \zeta$. Then the reflection coefficient equals zero and the impedance at the drum also equals: $Z_d = \zeta$. This is called perfect impedance match and is consistent with the following rule in physics. If the end impedance of a transmission line equals its characteristic impedance, then the transmission

line behaves as a reflection free, semi-infinitely long line.

[0047] The results above can easily be generalized to cases where one or more lumped elements are attached to the line. Assume that one stabilizer with a lumped impedance Z_S is placed at a distance *l* from the top. The impedance just below the stabilizer equals the sum of this lumped impedance and the line impedance just above the stabilizer, in mathematical terms:

$$Z_1 = Z_s + \frac{Z_0 \cos(kl) + j\zeta \sin(kl)}{\zeta \cos(kl) + jZ_0 \sin(kl)}\zeta \qquad (31)$$

[0048] This impedance can now be regarded as the end impedance seen by the line below it. If more than one stabilizer is used, the above formula must be used recursively by the following formula.

$$Z_i = Z_s(i) + \frac{Z_{i-1} \cos(kl_i) + j\zeta \sin(kl_i)}{\zeta \cos(kl_i) + jZ_{i-1} \sin(kl_i)}\zeta \qquad (31b)$$

where l_i is the distance between stabilizers *i*-1 and *i*, and Z_S (*i*) is the lumped impedance of stabilizer number ***i*** (not be confused with the partial impedance in equation (26)) . If there is only one stabilizer, the line impedance at the drum can be expressed by

$$Z_d = \frac{Z_1 \cos(kL - kl) + j\zeta \sin(kL - kl)}{\zeta \cos(kL - kl) + jZ_1 \sin(kL - kl)}\zeta \qquad (32)$$

[0049] If the fast sheave impedance is infinite, the above expression equals

$$Z_d = \frac{(Z_s + j\cot(kl)\zeta)\cos(kL - kl) + j\zeta \sin(kL - kl)}{\zeta \cos(kL - kl) + j(Z_s + j\cot(kl)\zeta)\sin(kL - kl)}\zeta \qquad (33)$$

[0050] This expression is valid also for a multi DOF damper where $Z_S = Z_{S,n}$ and $Z_{S,n}$ is found from the recursive formula (26) above.

[0051] Before discussing special cases it is worth noticing that the normalized impedance Z_d/ζ represents a response function describing how the dynamic line vibration is amplified in comparison with a line with no reflection at the top. More specifically, the dynamic fleet angle amplitude (in radians) at the drum resulting from an axial excitation speed v_a equals

$$\phi = \frac{F(-L)}{\zeta c} = \frac{Z_d}{\zeta}\frac{v_a}{c} \qquad (34)$$

[0052] It is not easy to see directly from the formula how this impedance varies but numerical examples below show that a stabilizer will change the drum impedance spectrum rather dramatically.

Special cases

[0053] Key parameters for most of the subsequent examples are the following. The special tension force is chosen for convenience, so that the wave propagation speed and the harmonic frequencies become round numbers. This tension force represents a typical line load when the hook load includes a drill string of moderate weight.

$T = 84.4kN$	tension force
$L = 50m$	fast line length
$2r = 0.0445m$	line diameter (1 ¾")
$m = 8.44kgm^{-1}$	specific line mass
$\tau = 2 \cdot 10^{-4}s$	internal bending loss time constant
$c = \sqrt{T/m} = 100ms^{-1}$	wave propagation speed
$\zeta = \sqrt{Tm} = 844Nsm^{-1}$	characteristic impedance (lossless case)
Data for an optional (1-DOF) stabilizer	
$M = 80kg$	mass (12% of the fast line mass $mL = 422kg$)
$B = 422Nsm^{-1} = 0.5\zeta$	damping coefficient (optional)
$l = 45m$	location ($0.1L$ above drum)

[0054] The modulus of the normalized line impedance at the drum position is visualized in figure 3 for three cases. The first case, represented by the dotted curve, is without any stabilizer. The resonance peaks in this case are integer multiples of the fundamental resonance frequency $f_1 = \Omega/2\pi = 1.0Hz$. The reduction of the peak heights with increasing frequency is a consequence of the bending induced damping, which increases rapidly with frequency. The logarithmic amplitude scale is used for visualizing the extreme differences in the dynamic line response. With the assumed internal line damping the response spans 5-6 orders of magnitude, from the maxima at the resonance frequencies to the minima at the anti-resonance frequencies. At the latter frequencies the force response is nearly zero, meaning that the line behaves as if it is not present.

[0055] The second case, the dashed-dotted curve, represents a stabilizer without damping. The stabilizer mass changes the line response dramatically. The most pronounced difference is that a new wide resonance peak appears at a frequency slightly higher than the 10^{th} harmonics of the stabilizer-less spectrum. This peak is the first one in a series of new, regularly spaced frequency peaks being the result of the mass being so close to the drum and so far away from the fixed fast sheave. We also see that the lowest line resonances are still there but they are shifted slightly to lower frequencies.

[0056] The third case, represented by the solid curve, is with added stabilizer damping. The extra damping reduces the lowest resonance peaks substantially, almost by a factor 50. In contrast the damping has only a small effect on the response above the new resonance peak. This can be explained by the fact that the high line damping makes the wave being reflected from the fast sheave is heavily attenuated when it reaches the stabilizer.

[0057] Case 2 (without damping) fairly well represents the impact on radial vibrations by the kind of stabilizer being used today. This is because there is virtually no friction restricting the stabilizer motion in the radial direction. The last case with damping is intended to simulate the action of current stabilizers on axial vibrations, although the effective level of the actual Coulomb friction is very uncertain.

[0058] It is interesting to see the effect of flipping the stabilizer position around the line centre. In the reference example above the distance from fast sheave to stabilizer equals l = 0.9L . Figure 4 shows the corresponding impedance spectra when l = 0.1L , which is much closer to the fast sheave. In this position the stabilizer has a much different effect on the line dynamics. The pronounced impedance peak between the original 10^{th} and 11^{th} harmonic observed with the low stabilizer is not seen any more. Without damping the new impedance spectrum is very much like the original spectrum, except that the frequencies are shifted slightly. When damping is added, the peak heights of the lowest resonances are very much reduced, to approximately 1% of the original height. Notice that the 10^{th} harmonic peak, which has a node at the stabilizer position, is virtually not affected by the stabilizer at all.

[0059] It can be seen that for frequencies making $|kl| << 1$ the line impedance above the stabilizer is $Z(-l) = -j\zeta \cot(kl) \approx T/(j\omega l)$. The last approximation equals the impedance of a linear spring with stiffness $S = T/l$. We can therefore deduce that perfect impedance match is obtained at the angular resonance frequency of the stabilizer

$$\omega = \sqrt{T/(lM)}$$

if the damping matches the characteristic line impedance, that is,

$$B = \zeta = \sqrt{T/m}$$

. Because the line has many resonance frequencies it may be more optimal to increase the damping beyond the characteristic impedance. The sacrifice of total impedance match at one particular frequency is outweighed by the better damping performance over a wider frequency band.

[0060] Reducing the stabilizer inertia is another way of reducing the resonance peaks in the band between the frequencies

$$\sqrt{T/(4\pi^2 lM)}$$

and

$$\sqrt{T/(4ml^2)}$$

. The mechanical mass can probably be decreased from today's typical value of 80 kg down to maybe half its value simply by a redesign of the roller assembly. The effect of such a reduction is visualized in figure 5. Notice that a mass reduction also increases the resonance frequency,

proportionally to
$1/\sqrt{M}$
.

[0061] The problem of poor damping of modes having a node close to the stabilizer location can be much reduced by using two stabilizers at different locations. Reference is made to figure 6 showing the effect of an extra dampener placed between the primary stabilizer and the fast sheave. In this case we have used an even higher linear damping ($B = 2\zeta$) for each pair of dampers. Also notice that the second stabilizer is purposely placed below the center location between the fast sheave and the first one. The main advantages of this location are 1) we avoid that the two locations represent neighbor nodes and poor damping at twice the original poor damping frequency and 2) both stabilizers will be exposed to nearly the same motion and force as the first one. Bear in mind that the effect of a stabilizer drops with the distance to the fast sheave.

Options for physical realizations and control levels

[0062] Below are listed some options for different realizations of dampers that may be used in stabilizers in hoisting systems according to the present invention. Later on a preferred option is described in more detail.

[0063] Schematic side view and top view of a hoisting system 1 according to the present invention is shown comprising a fast line 2 with a winch, here only shown as a drum 4, fast sheave 6 and stabilizer 8 are shown in figure 7. The use of two identical and perpendicular dampers 10 ensures equal damping in the two transversal directions. The roller assembly 14 is here shown with a double set of twin rollers 16 with V-shaped raceways 18, but other types of roller assemblies are possible, using other numbers (minimum 2) and shapes of rollers. Not shown in the schematic views is the anchoring of the telescopic dampers to the rig structure. The schematic drawings also lack means, typically a rod or wires, for keeping the vertical location of the roller assembly. If only two rollers are used, this guide rod may be substantially parallel to the line, sufficiently stiff and hinged with a universal joint near the fast sheave to allow transversal motions but prevent rotational motions of the roller assembly. The support structure to which the stabilizer and the wire rope guiding sheave are connected, is not shown in the figure.

[0064] The dampers 10, here visualized as small telescopic cylinders, can have three levels of control. These levels are discussed briefly below.

1) Passive damper

[0065] The term passive damper here means that it has fixed energy dissipation

characteristics. A candidate for such damper is a shock absorber used as in the suspension of automotive vehicles. A drawback of such shock absorbers is that they have rather non-linear and asymmetric characteristics. The asymmetry means that the damping force is different for compression speeds than for extensional speed. Another drawback is that vehicle shock absorbers seem to have a speed rating of typically 0.5 m/s, which is substantially lower than what may be needed in some embodiments of the present invention.

[0066] Another damper option is a balanced hydraulic cylinder, as shown schematically in figure 8. The damper 10 comprises a standard hydraulic cylinder 20 (hatched inner area representing oil) with hydraulic ports 22 in both ends. But instead of having only one piston rod it has two rods 24, 26 of equal diameters. Only the left one carries the axial load. The air filled cylinder to the right protects the dummy rod and carries the reactive load from the main cylinder. A not shown rubber bellow around the air exposed part of the left rod is recommended for protecting this rod too. The main advantages of this design are 1) the inner volume is constant thus creating zero extension force if a common pressure is applied in both chambers and 2) the damping characteristics are the same in both speed directions. When a transversal motion of the fast line makes the piston move, a resulting pressure difference across the piston will make the hydraulic fluid will flow partly through a fixed metering valve through the piston, and partly through an external bypass line of variable restriction. If simple metering orifices are used, the damping force will be nearly quadratic: $F \propto -v|v|$. This progressive non-linearity is probably far better that the other extreme non-linearity represented a Coulomb friction $F \propto -sign(v)$, because larger transversal line speed in general requires higher damping. If a more linear characteristics are highly desired, it is possible to use more advanced metering mechanisms, for instance, a variant found in some MC shock absorbers where a stack of thin plates are used at the end of the metering channels. When the pressure difference and flow rate increases, the stack is also lifted thus providing increased flow area and less restriction as compared with a constant orifice. Another possibility for linear characteristics of the external bypass line is to use either a single or a group of multiple parallel small cross section flow lines. If the flow in these lines is laminar, the pressure drop will increase proportionally with the flow rate. A drawback of this kind of linear behavior is that the fluid viscosity and thereby also the damping coefficient will be rather sensitive to the temperature.

2) Semi-active damper

[0067] The term semi-active means that the energy dissipating characteristics can be changed rather rapidly to adjust the damping characteristics dynamically. A possible candidate for such a damper is controllable shock absorbers found in some high end car brands, provided that the speed and force ratings are adequate. Key words are smart fluids and electric control of the damper characteristics. The most common smart fluid is magnetorheological fluids. As the name indicates, its viscous properties can be changed almost instantaneously by a magnetic field. It is mostly the gel strength and thereby the apparent Coulomb friction that can be controlled by the magnetic field. A high band width control of the rheology can, in principal at

least, be used to mimic a linear damper action. Because certain embodiments of the present invention may need to handle speed pulses of very short durations, actually down to 15 ms at maximum line speeds, it is questionable whether such a rapid control is feasible. A simpler option is to control the rheology more slowly in response to line tension, line speed and damper fluid temperature.

[0068] The balanced cylinder already mentioned as a passive damper option, could also be regarded as a semi-active damper, especially if it includes an external, controllable bypass valve in parallel with a metering orifice through the piston. The damping can be controlled in many ways. One of the simpler options is a stepwise flow resistance control, for instance by opening or closing one or more external bypass lines. A more advance option is to use an external metering valve that can be proportionally controlled to provide a continuous variation of the flow resistance. To allow for thermal expansion and also some small but finite leaks the oil volume should be connected to an external oil reservoir with an optional gas accumulator. This reservoir should preferably be connected to the center of the external bypass flow line to hinder an oscillating accumulator flow.

[0069] An alternative to hydraulic dampers is eddy current brakes. Such brakes have fairly linear characteristics, at least for moderate speeds and magnetization levels. It means that the braking force is proportional to the speed and to the stator current producing the magnetic field.

3) Active damper

[0070] Active damper here means an actuator that can handle two-way energy flow, not only energy dissipation. Both hydraulic and electric actuators can be used. Assume that the actuator itself can be represented by an inertia mass, M_C, so that the sum of the stabilizer and controller masses, $M_C + M_S$, is acted upon by the sum of the line force and the actuator controller force. Assume also that the controller is a general PID speed controller meaning that the controller force at angular frequency ω can be written as

$$F_c = \left(P + \frac{I}{j\omega} + j\omega D \right)\left(v_{set} - v\right) \equiv Z_c\left(v_{set} - v\right) \qquad (24)$$

[0071] The set speed, v_{set}, can either be set to zero, or to the fraction of the low pass filtered lateral speeds at the drum: $v_{r,lp}/L$ and $v_{a,lp}/L$. Notice that the integrator gain, I, has the dimension of linear stiffness whereas the derivative gain D has the dimension of mass.

[0072] The total, effective impedance of the stabilizer, including the mechanical stiffness $S = T/l$ is simply the sum of the mechanic impedance and the controller induced impedance. That is,

$$Z_{s,eff} = Z_s + Z_c = \left(P + B\right) + \frac{S + I}{j\omega} + j\omega\left(M_s + M_c + D\right) \qquad (25)$$

[0073] A normal PID controller has non-negative values for the factors for *I* and *D*, so at a first glance it seems optimal to use a P-controller only, where *P* is adjusted so that the total damping is approximately equal to the characteristic line impedance. That is,

$$P \approx \sqrt{Tm} - R \tag{26}$$

[0074] However, there is no rule stating that the integrator and derivative gain factors cannot be negative. Without such restrictions it is possible to achieve partially or even total impedance match over a wide frequency range by setting

$$I = -c_s S = -c_s \frac{T}{l} \tag{27}$$

$$D = -c_i (M_s + M_c) \tag{28}$$

where c_S and c_i are stiffness and inertia compensation factors, respectively. In practice, full compensation, c_S = 1 and c_i = 1, may not advisable, mainly because of the risk for instabilities. Stability problems can arise if there are time delays on the speed controller, or if the estimates for the mechanical stiffness (or tension) and masses have significant errors. However, partial compensation, up to 80-90% say, should be practically feasible if the time delays in the control loop are sufficiently low. By increasing the damping beyond the characteristic impedance, by a factor of 2 or 3 say, both the stability risk and the damping band width can be improved. These improvements are achieved on the expense of sacrificing a nearly full impedance match and high damping near the stabilizer resonance frequency.

[0075] The above controller impedance represents the ratio of telescopic force divided by telescopic speed. In practice, the basic moving element is a rotating motor connected to the linear motion by a gear mechanism. Such a motion converter, which could be a reduction gear combined with a ball screw or a rack and pinion mechanism, can be characterized by a transmission radius, r_c, being the ratio of linear speed to angular motor speed. It can be shown that the impedance for linear, telescopic motion is related to the angular motor axis impedance, Z_m , through

$$Z_c = \frac{Z_m}{r_c^2} \tag{29}$$

Generalization to oblique damper mounting

[0076] The examples above are worked out for the special case when the dampers are both normal to the line and mutual perpendicular. The results can be generalized to more general orientations of the dampers. Let α_1 and β_1 denote respective the deviations from pure radial and longitudinal directions for damper 1 having a telescopic impedance $Z_{c,1}$ and let α_2,β_2 and $Z_{c,2}$ be the corresponding parameters for damper 2. With longitudinal direction is here meant

the direction of line between center or rollers and the pivoting point at the top of the stabilizer bar. This direction may differ slightly from the longitudinal line direction.

[0077] It can be shown that the effective damper impedances in respective axial and radial directions can be written as

$$Z_a = Z_{s,a} + (\cos\alpha_1 \sin\beta_1)^2 Z_{c,1} + (\cos\alpha_2 \sin\beta_2)^2 Z_{c,2} \quad (30)$$

$$Z_r = Z_{s,r} + (\sin\alpha_1 \sin\beta_1)^2 Z_{c,1} + (\sin\alpha_2 \sin\beta_2)^2 Z_{c,2} \quad (31)$$

[0078] Here $Z_{s,a}$ and $Z_{s,r}$ represents the mechanical impedances of the roller assembly in axial and radial and directions, respectively. It is easily verified that the two expressions reduce to the first expression of equation (24) when $Z_{c,1} = Z_{c,2}$, $\beta_1 = \beta_2 = \pi/2$ and $\alpha_1 = -\alpha_2 = \pi/4$. Note that the latter angles represent the angles in the projected plane normal to the line axis and not in the plane spanned by the two dampers.

[0079] Using the angles $\alpha_1 = -\alpha_2 = \pi/4$ instead of $\alpha_1 = 0$ and $\alpha_2 = \pi/2$ represents several practical advantages. First, it makes it is easier to anchor both dampers to the rig structure. Second, each damper will get lower peak strokes, speeds and accelerations. The reduction factors for all these variables are approximately $\cos(\pi/4) = 0.71$. Third, it helps to distribute the wear of the telescopic damper almost evenly over its entire stroke. A damper exposed to the radial motion only ($\alpha = 0$) would have a small working range thereby making seal and rod wear much more concentrated.

[0080] A similar reduction of the telescopic stroke, speed and acceleration is obtained by a slant angle. Now the reduction factor is $\sin(\beta)$. A disadvantage of a small slant angle,$|\beta| << \pi/2$, is that the guide rod must handle an increasing longitudinal force equal to $F_t \cot\beta$, F_t being the resulting transversal force. If this rod is fastened to the roller assembly with an offset distance between its neutral axis and the fast line, then the force will also generate a bending moment being proportional to the offset and to the longitudinal force. The required rigidity and weight of the guide rod will therefore increase with decreasing slant angle.

The simulation model

[0081] A simulation model is developed both for supporting the linear theory above and for being able to calculate the effect a realistic stabilizers having non-linear damping characteristics. The model is based on the convective version of the wave equation (18). The convection, which means that the line is moving longitudinally with a constant translation speed V , is obtained by substituting the partial time derivatives by the so-called material derivatives: $\partial / \partial t \rightarrow \partial / \partial t + V \cdot \partial / \partial x$. Numerical solutions are obtained by representing the string by typically 200 discrete elements each with a mass $\Delta M = m\Delta L$, ΔL being the constant element length. The end nodes, representing the drum and fast sheaves, are modelled with nearly infinite masses

to prevent force induced lateral motion. The stabilizer node is also specially treated with a mass $\Delta M + M_S$ and a speed dependent external damping force. The force is, in general, non-linear and represented by the formula

$$F_d = -D_{s\varepsilon} \cdot |v_s|^{\varepsilon-1} v_s \approx -D_{s\varepsilon} \cdot \left(v_s^2 + v_0^2\right)^{(\varepsilon-1)/2} v_s \quad (32)$$

where $D_{s\varepsilon}$ is a generalized damping coefficient representing the damping force at a stabilizer speed of $v_S = 1 m/s$, ε is a speed exponent and v_0 is a small transition speed (typically 0.01 m/s) included for numerical reasons. This speed exponent equals 1 for linear damping, 0 for Coulomb friction and 2 for a quadratic damping but it can have any value between the two last extremes.

[0082] It is useful to explore the damping of the balanced hydraulic cylinder visualized in figure 8 and also being suggested as a working embodiment. Assume that the hydraulic oil is forced to flow through an internal and/or external restriction and that the restriction creates a pressure drop described by the Bernoulli equation

$$\Delta p = \frac{1}{2}\rho |v_m| v_m = \frac{1}{2}\rho \frac{A_h^2}{A_m^2} |v_s| v_s \quad (33)$$

where $v_m = v_S A_h / A_m$ is the speed of the fluid through the metering restriction, A_h is the hydraulic cylinder area and A_m is the effective cross section area of the metering restrictions. The corresponding damping force is simply

$$F_d = -A_h \Delta p = -\frac{1}{2}\rho \frac{A_h^3}{A_m^2} |v_s| v_s = -D_{s2} |v_s| v_s \quad (34)$$

[0083] The last equation can be used for finding the metering cross section as a function of the hydraulic area and the chosen damping coefficient D_{s2} :

$$A_m = \left(\frac{\rho A_h^3}{2 D_{s2}}\right)^{1/2} \quad (35)$$

[0084] The simulation model is implemented in Simulink, a powerful simulation tool under the Matlab umbrella. Examples of simulation results are shown in figures 9 and 10, representing the respective cases without any stabilizer and with one stabilizer having two identical dampers mounted as visualized in figure 7. The line parameters are the same as in the numerical example used for the linear analysis. Each damper is a passive hydraulic one as visualized in figure 8. The total mass of the roller assembly and the stabilizer is 40 kg and the quadratic damper coefficient is

$D_{s2} = 4000\, N/(m/s)^2 = 4.7\, \zeta/(m/s)$.

[0085] Both cases cover a simulation time window of 16 seconds where the drum starts at rest at the beginning of layer 2 and accelerates to a steady rotation speed of approximately $\Omega \approx 4 \cdot 2\pi s^{-1} = 240 rpm$. Approximately means that the actual speed is purposely reduced by the resonance shift factor 1- $(v/c)^2 \approx 0.97$ due to the longitudinal line speed of $v \approx 15.7 m/s$. The

selected speed corresponds to line excitation frequencies being multiples of the cross-over frequency $f_{x0} \approx 2\Omega/2\pi = 8.0Hz$. This frequency is the 8^{th} harmonics of the theoretically predicted line resonances, see figure 4. The simulation model confirms that the above shift factor is correct, because resonances are not hit spot on if the frequency shift factor is neglected for the high line speeds.

[0086] The simulation results basically confirm what was predicted by linear theory. When the cross-over frequency hits a line resonance, large vibrations build up in the line. The sharp resonances predicted by the linear theory also imply that it takes time to reach steady state vibrations. With reference to figure 9 we see that steady state is not completely reached before the drum spooling enters layer 3 and the excitation direction reverses. This sudden polarity reversal of speed excitation pulses explains why the dynamic line vibrations temporarily reduce when the spooling starts on the 3^{rd} layer. Simulation with extended time intervals, not shown here, show that the severe line vibrations pick up again beyond 16 s.

[0087] Similar simulations are also carried out with one stabilizer (having two perpendicular dampers) placed near the fast-sheave, see figure 10. When comparing with the previous results (without any stabilizer figure 9) we observe that vibrations are now much smaller in amplitude. Additional simulation results, not visualized in graphs here, show the following:

1. 1. The vibration reduction is surprisingly robust against changing in changes of the damping characteristics. Only minor changes in the peak fleet angle are observed if the quadratic damping coefficient is increased or reduced by a factor of 2. Moreover, switching from quadratic to linear damping characteristics also seems to have a surprisingly small effect on the peak acceleration, provided that the damping force magnitudes at typical transversal speeds around 1 m/s is roughly the same in both cases.
2. 2. The simulator confirms the big difference in response predicted by figures 3 and 4 when the stabilizer position is flipped. When the stabilizer is placed a distance 5 m from the drum, high resonance vibrations are seen for drum speeds having a harmonics frequency that matching the predicted resonance at about 10.8 Hz.
3. 3. When the damping is non-linear, the dynamic line vibrations and axial fleet angles are not independent on the stabilizer orientation α_1 even though the two identical stabilizers are identical and perpendicular ($\alpha_1 - \alpha_2 = \pi/2$). This is because combined motions in the stabilizer directions have different patterns and peak values, as visualized in the speed subplots in figures 1 and 2.
4. 4. The input speed and acceleration at the drum end of the line are independent of the line dynamics. In contrast, the corresponding variables at the stabilizer are very sensitive to the stabilizer mass and damping characteristics. In the examples above the axial peak speed were reduced by a factor 6, from $3.36m/s$ and for the non-stabilized case to $0.56m/s$ for the stabilized case. The corresponding figures for the axial acceleration are 29.0g and 3.4g.
5. 5. The simulation model also provides values for the stabilizer force and for the

dissipated power. In the enclosed case the peak force were 1450 N while the peak power is in the order of a few hundred watts. The low pass filtered power is far less, in the order of 30W, which represents only a marginal heating of the hydraulic cylinder.

6. 6. The stabilizer, when placed relatively close to the fast sheave, has virtually no effect when the fundamental excitation frequency (the double drum rotation frequency) hits a resonance having a node at the stabilizer location. It is therefore recommended to choose an even shorter distance between the fast sheave and the stabilizer so that it is less than half the wave length for the combination of empty block line tension and maximum drum speed. Alternatively, one can use two stabilizers as discussed below.
7. 7. Simulations with two stabilizers, each with two perpendicular dampers with a relatively high damping ($M_1 = M_2 = 40kg;\ B_1 = B_2 = 2\zeta$), mounted at different locations ($z_1 = -0.1L$ and $z_2 = 2z_1/3$) strongly indicate that the vibration damping can be substantially improved as compared with the single stabilizer solution discussed here. Especially the poor damping of modes having a node at the first location is very much improved. This improvement confirms what was predicted by the impedance spectrum for dual stabilizers visualized as the solid curve in figure 6.

An example of a working embodiment

[0088] A preferred set of fast line dampers are two balanced hydraulic cylinders as visualized and mounted in figure 7, right and left, respectively. Key parameters for the roller assembly and cylinders are

$M_s = 40kg$	effective stabilizer mass (roller assembly + rods + piston)
$l = 0.10L$	Distance between damper and fast sheave (tangent point)
$L_d = 0.6m$	Length of damper (in center position, 50 % extended)
$\Delta L_c = 0.2m$	Maximum stroke
$\alpha_1 = -\alpha_2 = \pi/4$	Azimuth angles (relative to the pure radial direction)
$\beta_1 = \beta_2 = \pi/2$	Inclination angles (relative to the line direction)
$A_h = 884mm^2$	Hydraulic area (from $D_{rod} = 30mm$ and $D_{cyl} = 45mm$)
$\varepsilon = 2$	speed exponent (quadratic damping)
$D_{s2} = 4000\ Ns/(m/s)^{\varepsilon}$	damping coefficient

[0089] The chosen damping coefficient corresponds to a restriction area of $A_m = 8.66mm^2$, calculated from equation (35) when using a fluid density of $\rho = 870kg/m^3$.

[0090] A typical drum length (width) is X_d = 2.0m so the chosen stroke can easily handle a damper position of maximum l = 0.10L below the fast sheave. This is because the total theoretical stroke for both dampers will be cos $\alpha \cdot X_d\, l/L$ = 0.14m . The suggested cylinder and piston rod diameters correspond to a hydraulic area of A_h = 884mm^2, which in turn corresponds to a pressure of $\Delta p \approx 5.6 MP\alpha$ at an estimated maximum damping force of $F \approx 5kN$. This is far below a standard pressure rating $\Delta p \approx 21 MP\alpha$ (or 3000 psi). Standard hydraulic fittings and seals are therefore applicable.

[0091] The suggested metering area represents a progressive damping. Assuming that the Bernoulli equation for pressure drop applies, that is, $\Delta p \approx 0.5\rho|v_m|v_m$ where $p \approx 850 kgm^{-3}$ is the hydraulic fluid density and $v_m = v_d A_d/A_m$ is the fluid speed through the metering nozzle in the case when the external bypass is closed. The corresponding effective impedance or force to speed ratio then becomes

$$F/v_d = \Delta p A_d/v_d \approx 0.5\rho|v_d|A_d^3/A_m^2$$

. With the suggested dimensions and a telescopic damper speed of v_d = 1.0ms^{-1} this ratio becomes $F/v_d \approx 2900 Nsm^{-1}$. This value is about 4.5 times the characteristic impedance of a 1.75" fastline exposed to a tension of 50 kN. If the external bypass loop is opened, the total bypass area is up to tripled and the effective impedance at the same speed is reduced by a factor from 1 to 1/9, the latter representing a damping less than the characteristic impedance. With reference to the theory above it is anticipated that these dampers will reduce the fastline vibrations substantially. If the external restriction is adjusted manually, the dampers can be regarded as passive. In contrast, if the restriction is varied automatically in response to the drum speed and line tension for achieving optimal damping characteristics over a wide range of operational conditions, then the dampers can be classified as semi-active.

[0092] The roller assembly, which connects the dampers to the fast line, is not discussed in details here because there are many designs that will work almost equally well. The suggested variant in figure 5 can probably be designed to a mass of less than 30 kg resulting in a total mass of one dampener less than 40 kg. To minimize noise from the relatively small rollers to the dampers and rig structure it is advisable to use elastomer (rubber) sleeves in the couplings, similar to those used in many vehicle shock absorbers. Such coupling will act as mechanical low pass filter reducing transfer of high frequency vibration components and transmitting mainly the low frequency components. Noise reduction and smoother roll action can also be obtained by substituting parts of the V-profile of the rollers by a U-profile having a curvature radius matching the maximum radius of the line.

REFERENCES CITED IN THE DESCRIPTION

Cited references

Patent documents cited in the description

- US2565693A [0003]
- PL158970B1 [0003]
- US2015353331A1 [0003]
- WO2014209131A [0008]

Patentkrav

1. Hejsesystem (1) til en borerig, hvilket hejsesystem (1) omfatter:

- en wire (2);
- et spil (4) til at trække wiren (2) ind og føre den ud,
- en støttestruktur, såsom et boretårn;
- en wireføringsskive (6), der er forbundet med støttestrukturen, hvilken wireføringsskive (6) er tilvejebragt mellem spillet og et lastophængningselement langs med wiren (2); og
- én eller to stabilisatorer (8) til dæmpning af sidevibrationer af wiren (2) mellem spillet (4) og wireføringsskiven, **kendetegnet ved**, at for at øge den ene eller to stabilisatorers (8) dæmpningseffekt er hver af den ene eller de to stabilisatorer (8) tilvejebragt tættere på wireføringsskiven (6) end på spillet (4) langs med wiren (2),

hvor en første stabilisator (8) af den ene eller de to stabilisatorer (8) omfatter én eller flere dæmpere (10) med første ende(r) forbundet med støttestrukturen, hvor den første stabilisator (8) endvidere omfatter et eller flere par føringsruller (16), der er fælles for hver af den ene eller flere dæmpere og forbundet med en anden ende af det ene eller flere par af dæmpere (10), hvor wiren (2) er tilpasset til at løbe mellem rullerne (16) af hvert at det ene eller flere par af føringsruller, og

hvor den første stabilisator (8) omfatter et par dæmpere (10), hvor de to dæmperes længdeakser i alt væsentligt er orienteret vinkelret på hinanden.

2. Hejsesystem (1) ifølge krav 1, hvor hver af de i alt væsentlig vinkelret orienterede dæmpere (10) er tilvejebragt ved henholdsvis ± $\pi/4$ radianer i forhold til den radiale retning af en spiltromle i spillet (4) i et plan vinkelret på wirens længdeakse.

3. Hejsesystem (1) ifølge et hvilket som helst af kravene 1-2, hvor den ene eller flere dæmpere (10) er passive dæmpere med i alt væsentligt ikke-justerbare

dæmpningsegenskaber.

4. Hejsesystem (1) ifølge et hvilket som helst af kravene 1-2, hvor den ene en eller flere dæmpere (10) er semiaktive dæmpere med styrbare energidissiperende egenskaber.

5. Hejsesystem (1) ifølge et hvilket som helst af kravene 1-2, hvor den ene eller flere dæmpere (10) er aktive dæmpere med styrbare dæmpningsegenskaber og styrbar, aktiv reaktion.

6. Hejsesystem (1) ifølge et hvilket som helst af de foregående krav, hvori hejsesystemet omfatter to stabilisatorer (8), hvor en anden stabilisator fortrinsvis er tilvejebragt mellem wireføringsskiven (6) og den første stabilisator (8) langs med wiren (2), og endnu mere fortrinsvis mellem wireføringsskiven (6) og den første stabilisator (8) tættere på den første stabilisator (8) end på wireføringsskiven (6) langs med wiren (2).

7. Hejsesystem (1) ifølge et hvilket som helst af de foregående krav, hvor den første og potentielt anden stabilisator (8) har en bevægelig masse i størrelsesordenen 12 procent eller mindre af en fast line-masse, fortrinsvis 6 procent eller mindre.

8. Hejsesystem (1) ifølge et hvilket som helst af de foregående krav, hvor den første stabilisator (8) er tilvejebragt i størrelsesordenen 1/10 af afstanden fra wireføringsskiven (2) til spillet (4).

9. Borerig omfattende et hejsesystem (1) ifølge krav 1.

10. Borerig ifølge krav 9, hvilken borerig endvidere omfatter:

- midler til at måle omdrejningshastigheden for en spiltromle i spillet (4);
- midler til at måle spændingen i wiren (2) mellem spiltromlen og wireføringsskiven (6);
- en styreenhed indrettet til at modtage den målte rotationshastighed og den målte spænding.

11. Borerig ifølge krav 10, hvor styreenheden er tilpasset til at bruge den målte spiltromle-rotationshastighed og wirespændingen som input i en model til beregning af optimerede egenskaber for den første og/eller anden stabilisator, hvor styreenheden, hvis den første og/eller anden stabilisator er af semiaktiv eller aktiv type, endvidere er tilpasset til at justere bevægelsesegenskaberne for den første og/eller anden dæmper.

12. Fremgangsmåde til dæmpning af sidevibrationer i en wire (2) ved hjælp af et hejsesystem (1) ifølge krav 1, hvor fremgangsmåden omfatter følgende trin:

- midler til at måle omdrejningshastigheden for en spiltromle i spillet (4);
- måling af wirens (2) spænding mellem spillet (4) og wireføringsskiven (6); og
- beregning af optimerede bevægelsesegenskaber for at reducere de laterale vibrationer for én eller flere dæmpere (10) af den første stabilisator (8) baseret på den målte rotationshastighed og spænding.

13. Fremgangsmåde ifølge krav 12, hvor fremgangsmåden, hvis dæmperne (10) er af en semiaktiv eller aktiv type, endvidere omfatter:

- justering af dæmpernes (10) bevægelsesegenskaber baseret på de beregnede, optimerede bevægelsesegenskaber.

DRAWINGS

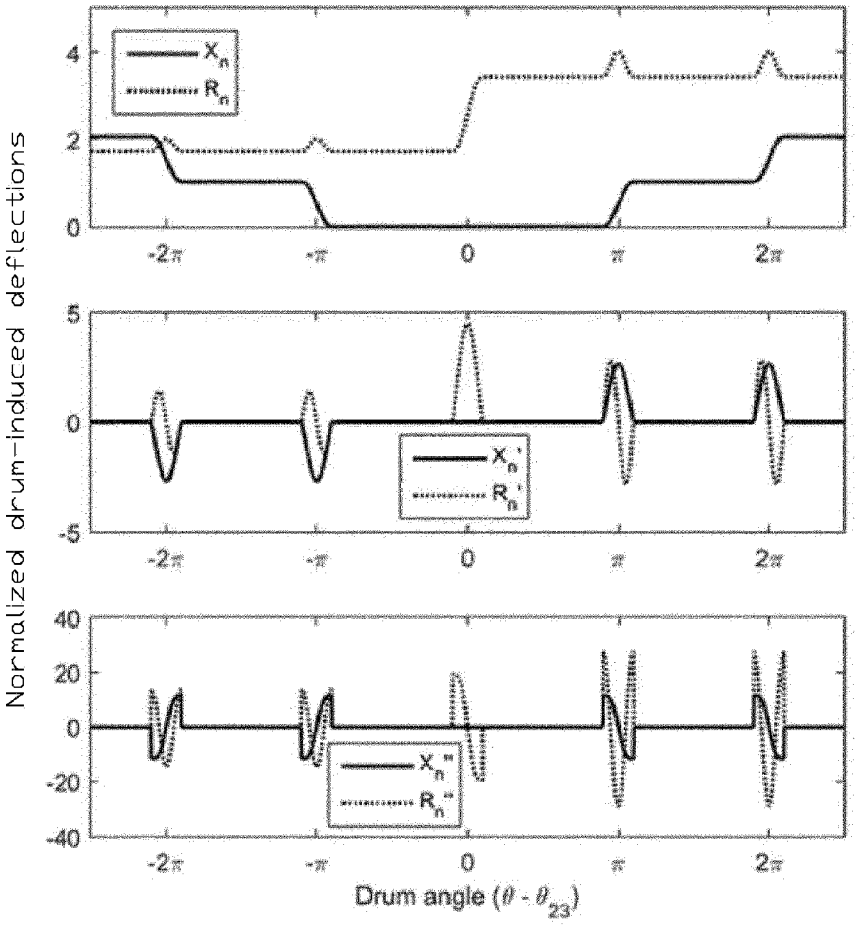

Fig. 1

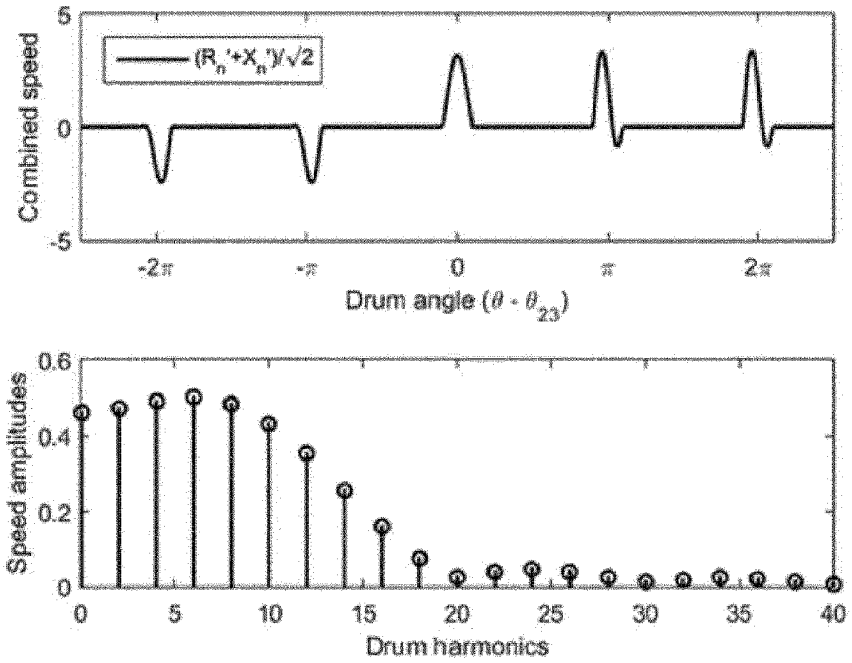
Combined speed
$(R_n'+X_n')/\sqrt{2}$
5
0
-5
-2π
-π
0
π
2π
Drum angle ($\theta - \theta_{23}$)
Speed amplitudes
0.6
0.4
0.2
0
0
5
10
15
20
25
30
35
40
Drum harmonics

Fig. 2

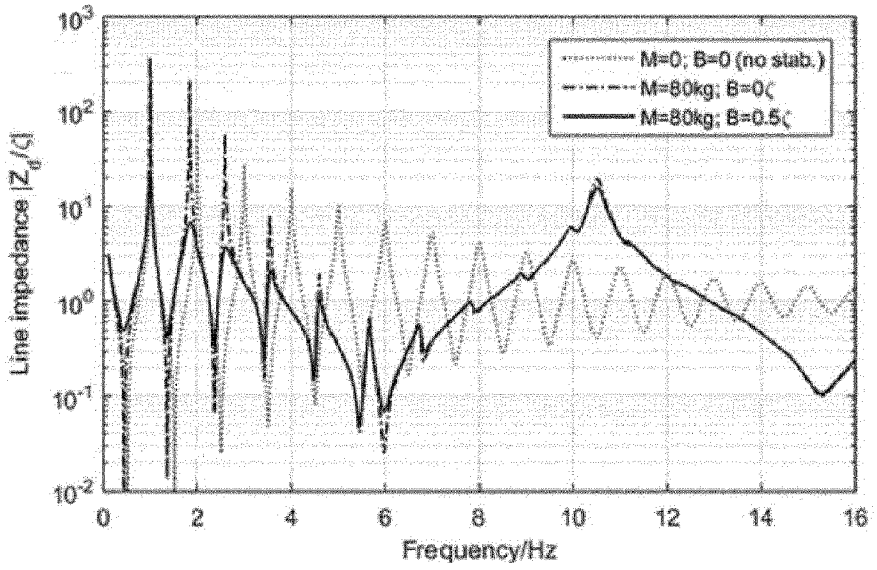
M=0; B=0 (no stab.)
M=80kg; B=0ζ
M=80kg; B=0.5ζ
Line impedance |Z_θ/ζ|
Frequency/Hz
10^3
10^2
10^1
10^0
10^-1
10^-2
0
2
4
6
8
10
12
14
16

Fig. 3

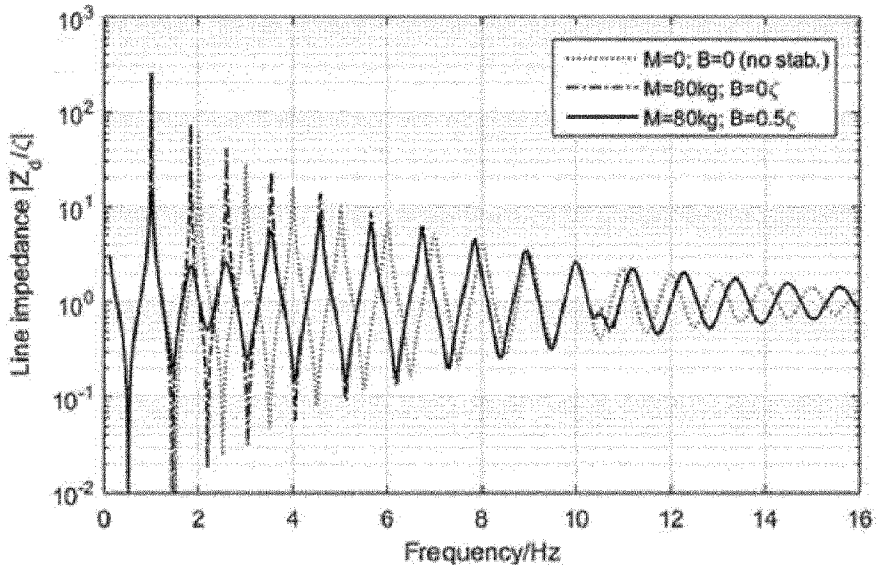
M=0; B=0 (no stab.)
M=80kg; B=0ζ
M=80kg; B=0.5ζ
Line impedance |Z_d/ζ|
Frequency/Hz
10^3
10^2
10^1
10^0
10^-1
10^-2
0
2
4
6
8
10
12
14
16

Fig. 4

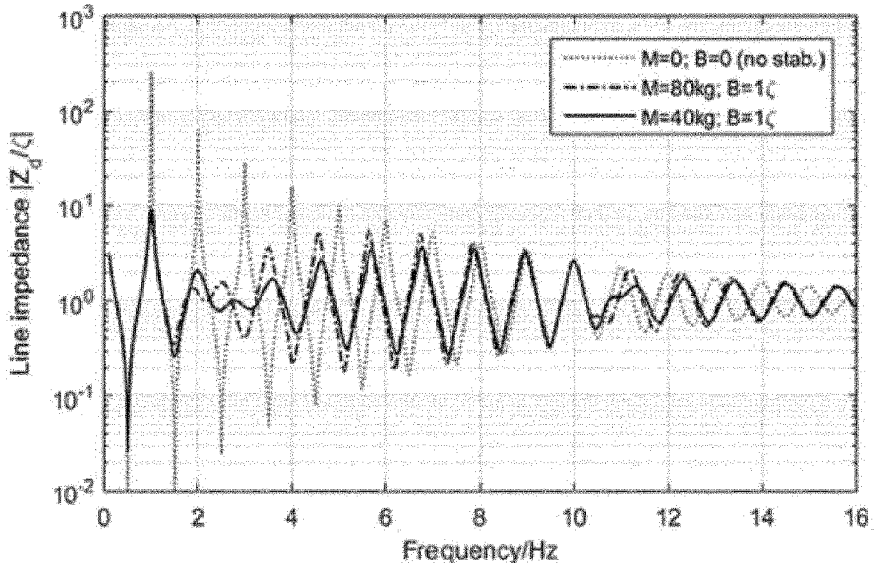
M=0; B=0 (no stab.)
M=80kg; B=1ζ
M=40kg; B=1ζ
Line impedance |Z_d/ζ|
Frequency/Hz
10^3
10^2
10^1
10^0
10^-1
10^-2
0
2
4
6
8
10
12
14
16

Fig. 5

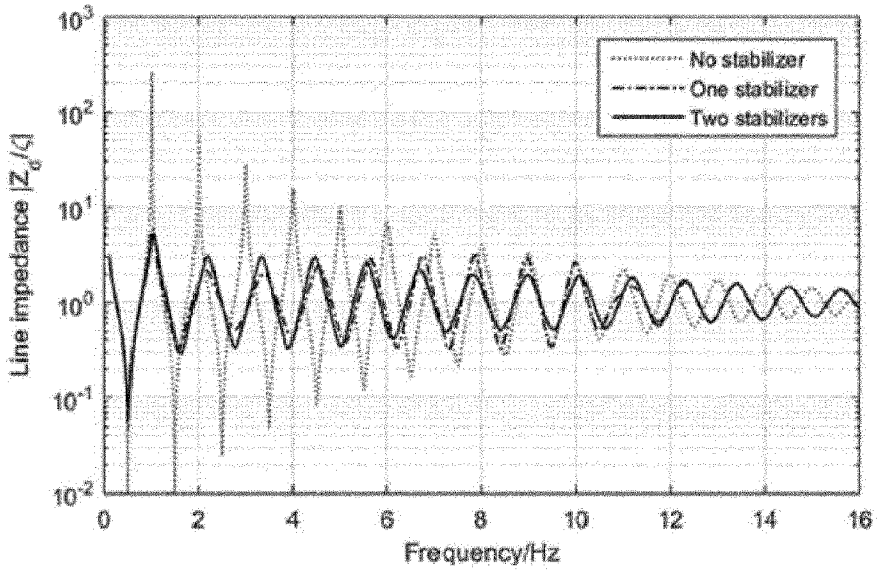
No stabilizer
One stabilizer
Two stabilizers
Line impedance |Z_d/Ω|
Frequency/Hz
10^3
10^2
10^1
10^0
10^-1
10^-2
0
2
4
6
8
10
12
14
16

Fig. 6

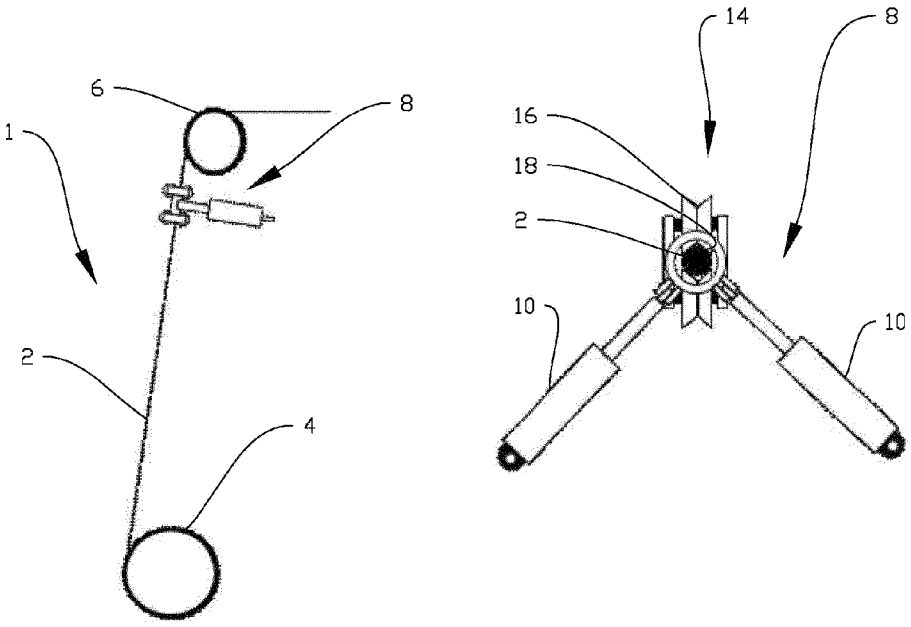

Fig. 7

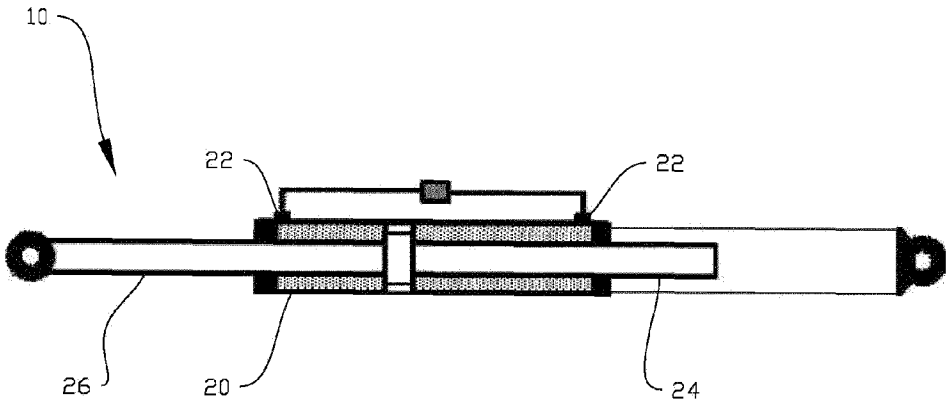

Fig. 8

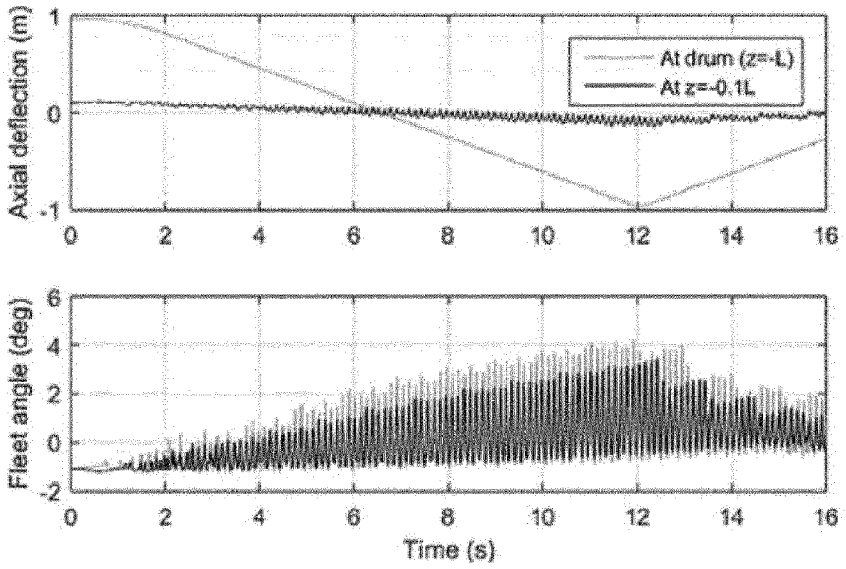
Axial deflection (m)
1
0
-1
0
2
4
6
8
10
12
14
16
At drum (z=-L)
At z=-0.1L
Fleet angle (deg)
6
4
2
0
-2
0
2
4
6
8
10
12
14
16
Time (s)

Fig. 9

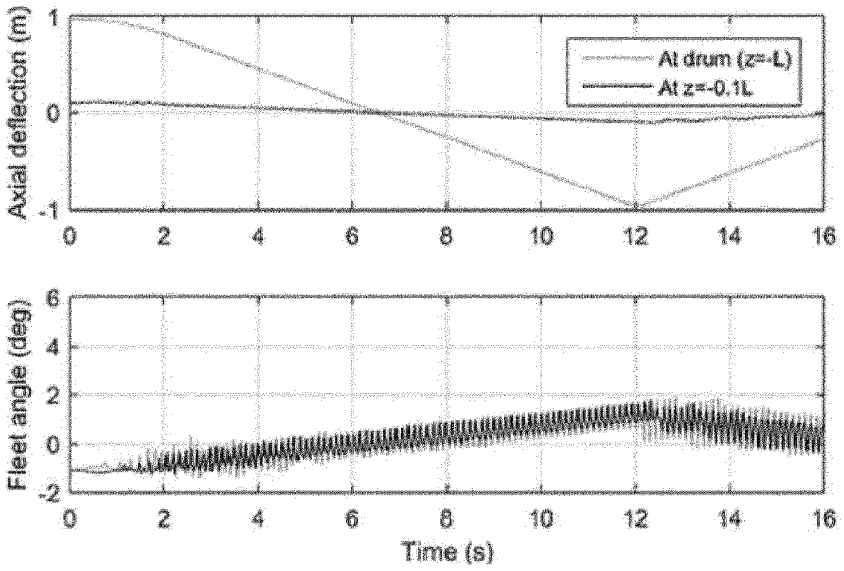
Axial deflection (m)
1
0
-1
0
2
4
6
8
10
12
14
16
At drum (z=-L)
At z=-0.1L
Fleet angle (deg)
6
4
2
0
-2
0
2
4
6
8
10
12
14
16
Time (s)

Fig. 10